Sensors & Actuators: B. Chemical 376 (2023) 133001

Contents lists available at ScienceDirect

Sensors and Actuators: B. Chemical

journal homepage: www.elsevier.com/locate/snb

# QRsens: Dual-purpose quick response code with built-in colorimetric sensors

Pablo Escobedo [a,b,*,1], Celia E. Ramos-Lorente [b,c,1], Ammara Ejaz [d], Miguel M. Erenas [b,c], Antonio Martínez-Olmos [a,b], Miguel A. Carvajal [a,b,e], Carlos García-Núñez [d], Ignacio de Orbe-Payá [b,c], Luis F. Capitán-Vallvey [b,c], Alberto J. Palma [a,b,e,*]

[a] Electronic and Chemical Sensing Solutions (ECsens), CITIC-UGR, Department of Electronics and Computer Technology, University of Granada (UGR), Granada 18071, Spain
[b] Unit of Excellence in Chemistry Applied to Biomedicine and the Environment of the University of Granada, Granada, Spain
[c] Electronic and Chemical Sensing Solutions (ECsens), Department of Analytical Chemistry, University of Granada (UGR), Granada 18071, Spain
[d] Scottish Universities Physics Alliance (SUPA), Institute of Thin Films, Sensors & Imaging (TFSI), University of the West of Scotland (UWS), Paisley PA1 2BE, United Kingdom
[e] Sport and Health University Research Institute (iMUDS), University of Granada (UGR), Granada 18071, Spain

ARTICLE INFO

*Keywords:*
QR code
Colorimetric sensors
Colour correction
Smartphone
QR analytical devices

ABSTRACT

QRsens represents a family of Quick Response (QR) sensing codes for in-situ air analysis with a customized smartphone application to simultaneously read the QR code and the colorimetric sensors. Five colorimetric sensors (temperature, relative humidity (RH), and three gas sensors ($CO_2$, $NH_3$ and $H_2S$)) were designed with the aim of proposing two end-use applications for ambient analysis, i.e., enclosed spaces monitoring, and smart packaging. Both QR code and colorimetric sensing inks were deposited by standard screen printing on white paper. To ensure minimal ambient light dependence of QRsens during the real-time analysis, the smartphone application was programmed for an effective colour correction procedure based on black and white references for three standard illumination temperatures (3000, 4000 and 5000 K). Depending on the type of sensor being analysed, this integration achieved a reduction of ~71 – 87% of QRsens's dependence on the light temperature. After the illumination colour correction, colorimetric gas sensors exhibited a detection range of 0.7–4.1%, 0.7–7.5 ppm, and 0.13–0.7 ppm for $CO_2$, $NH_3$ and $H_2S$, respectively. In summary, the study presents an affordable built-in multi-sensing platform in the form of QRsens for in-situ monitoring with potential in different types of ambient air analysis applications.

## 1. Introduction

Quick Response (QR) codes emerged in the 1990 s with additional advantages over traditional barcodes such as the possibility of encoding (storing) a greater volume of information, being faster and easier to read, and the ability to be digitally scanned through a smartphone camera [1]. A traditional QR code is a two-dimensional matrix with several small blocks arranged in a square-shaped grid with three large squares in the corner for position detection, size, angle, and outer shape recognition. Upon scanning a QR code, the reader (e.g., a smartphone) initially identifies these three squares' patterns and then reads the encoded information within it in all directions. QR codes were initially designed for inventory tracking in vehicle parts manufacturing [2], however, their use has expanded to products quality control, life cycle management, supply chain management, in the media (e.g., TV shows and newspapers) and to store Uniform Resource Locators (URLs) or other custom identifiers (e.g., the COVID-19 vaccination certificate). QR codes are also widely used in distinct areas of daily life such as education [3], health [4,5], nutrition [6,7], entertainment and culture [8,9], commerce [10], and security [11], among others [12–14]. The epidemic use of smartphones enables QR codes as a potential gateway to the Internet of Things (IoT) within the reach of any individual user [15].

* Corresponding authors at: Electronic and Chemical Sensing Solutions (ECsens), CITIC-UGR, Department of Electronics and Computer Technology, University of Granada (UGR), Granada 18071, Spain.
*E-mail addresses:* pabloescobedo@ugr.es (P. Escobedo), ajpalma@ugr.es (A.J. Palma).
[1] These author contributed equally to this work.

https://doi.org/10.1016/j.snb.2022.133001
Received 29 July 2022; Received in revised form 10 November 2022; Accepted 14 November 2022
Available online 17 November 2022

In this context, herein we present QRsens, an enhanced QR code with built-in colorimetric sensors. The general concept of the developed system is shown in Fig. 1 and Supplementary Movie. Taking advantage of a traditional QR code anatomy, the three-positioned corners of the QR code have been replaced by circle-shaped colorimetric sensors [16]. In combination with a custom-developed smartphone application where image processing of QRsens is conducted, multiple sensing capabilities have been added to standard QR codes while retaining its original purpose as data storage systems. QRsens codes were fabricated by screen printing technology in a white paper substrate using a commercially available two-component thermochromic ink and custom-developed sensing inks for relative humidity (RH), carbon dioxide ($CO_2$), ammonia ($NH_3$), and hydrogen sulphide ($H_2S$). The colour change of the sensors was characterised by the evaluation of the hue (H) or saturation (S) values in the HSV colour space, captured and automatically processed through the developed smartphone application. By combining three of these five sensors, two versions of QRsens codes are proposed in this work, aimed at two end-use applications: enclosed spaces monitoring (temperature, RH, and $CO_2$ sensors) and smart packaging applications ($H_2S$, $NH_3$, and $CO_2$ sensors). Additionally, two black and white (B/W) references are printed in the centre of QRsens to conduct automatic colour correction of environmental light conditions for the detected colorimetric sensors during the image processing pipeline. Although other developments of QR-like codes with colorimetric sensors can be found in the literature, the proposed device make use of five sensors (that can be combined into groups of three) that have never been simultaneously proposed in other solutions. Additionally, the presented system distinguishes from previous works by combining the following aspects simultaneously: *i)* QRsens can be manufactured using standard fabrication techniques, i.e., screen-printing; *ii)* The QR code still maintains its original functionality as data storage device; *iii)* It implements an automatic light colour correction technique; and *iv)* An ad-hoc smartphone application has been developed implementing automatic image processing for sensor detection and colour correction, data storage, and results sharing. The comparison with other systems is shown below in more detail in Table 3 of the Results and Discussion section.

Supplementary material related to this article can be found online at doi:10.1016/j.snb.2022.133001.

The proposed applications of QRsens are based on the sensor's combination in each case. For instance, $NH_3$ detection can be used as a "freshness label" for smart food packaging applications due to its natural release from protein degradation. $NH_3$ detection is well suited for spoilage detection in protein-rich foods such as meat, fish, and vegetables [17,18]. In the case of $H_2S$, it is a volatile gas mainly produced during the degradation process of the sulphur-containing amino acids, so it is a characteristic compound to assess meat spoilage [19,20] as well. $CO_2$ inside food packages is also a key parameter to control in modified atmosphere packaging (MAP) applications to create a protective atmosphere surrounding the food, with the aim to decrease microbial growth rate and therefore extend the shelf life of the packed food [21]. Typically, $CO_2$ is flushed into the package to obtain concentrations above 60% [22]. In this context, QRsens could inform of a leakage in the package if $CO_2$ concentration falls drastically below this threshold. In any case, it is worth mentioning that for smart packaging applications the QRsens code would be placed inside the package to be monitored, which is a typical requirement in this type of systems [19,21,22]. In that case, it would be necessary to study migration of dyes, toxicity of chemicals, etc. Additionally, the package must be optically transparent as it is common in most of food packages. Likewise, $CO_2$ monitoring can also be useful in health-related applications. It is well known that normal atmospheric air levels (~0.04%) are not harmful, however, a continuous accumulation of $CO_2$ in confined spaces becomes a potential danger to human health. Some studies have related prolonged $CO_2$ inhalation in indoor environments to symptoms of discomfort, fatigue, dyspnoea, dizziness, headache, sweating, muscular weakness, and drowsiness [23,24]. In this case, QRsens could serve as a threshold detector if $CO_2$ exceeds safety limits. Along with air quality, temperature and RH can also be associated with indoor microbial exposure, which is related to adverse pulmonary health effects [25]. Additionally, many recent studies have also connected these three parameters with SARS-CoV-2 transmission [26–28]. It is worth mentioning that other QRsens codes could be proposed using different combinations of the colorimetric sensors, or alternative applications could also be targeted using the same sensors. For instance, temperature and RH can be also related to food spoilage [29]. Likewise, $NH_3$ and $H_2S$ monitoring also have high relevance in terms of environmental safety [30,31].

## 2. Materials and methods

### 2.1. QRsens design and fabrication

QRsens was designed to simultaneously have dual functionality: (*i*) as a standard QR code to store custom information, and (*ii*) as a sensing platform with up to three colorimetric-based sensing elements. Such sensing elements have been integrated into the QR code taking advantage of the structure and components of the code itself, thus enhancing the functionality of the original QR code design without affecting its main purpose as a data storage device. In essence, QRsens benefits from the anatomy of a standard QR code to add the sensing functionalities, in particular from the position markers, i.e. the three large square patterns

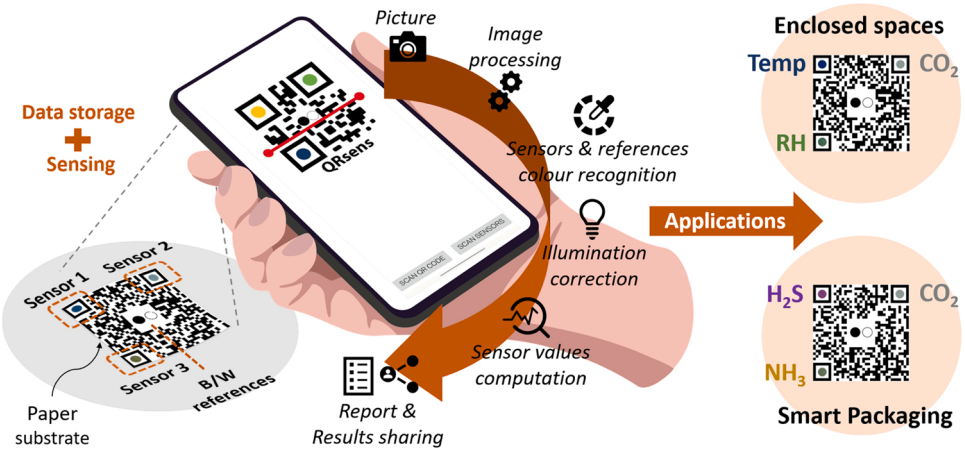


**Fig. 1.** System overview and concept of QRsens, which consists of a QR code with integrated colorimetric sensors in combination with a custom-developed smartphone application for the acquisition and automatic processing of QRsens. Two different end-use applications are proposed by combining three of the five custom-developed sensors: enclosed spaces monitoring (temperature, RH, and $CO_2$) and smart packaging sensing ($H_2S$, $NH_3$, and $CO_2$).

in the corners of the code used for detecting its position, size, angle and outer shape [1]. The inside code consisting of several small blocks where the information is encoded is kept unaltered, so the QR code continues to serve its original purpose. Additionally, QRsens takes advantage of two design aspects of standard QR codes: (*i*) the inner eyes of the position patterns (see Fig. 2a) can take other shapes different from the traditional square shape; and (*ii*) a free area or empty space can be left in the centre of the code, normally used to place any custom image or logo. In this way, the three inner eyes of the position patterns are replaced by the corresponding three circular-shaped colorimetric sensors, while the empty space in the centre is used to locate two additional circles -the black and white (B/W) references- for light colour correction during the image processing pipeline. The reason for the circular shape of the sensors and the B/W references is related to the image processing conducted in the developed smartphone application (see details in Section 2.2.1). Furthermore, the area in the QR code that contains the data (for example, an URL) is extended to also encode the information about which sensor is placed in each corner of the QRsens code. Following this approach, when the user reads the code with the custom smartphone application, such information regarding the sensors is automatically detected and separated from the original information of the QR code (e.g., the URL), so the process is transparent for the end-user and QRsens is self-contained with respect to its sensing functionality. To that end, information about the sensors is placed before the original data using specific keywords separated by semicolons, as detailed below. A visual summary of the design process from a standard original QR code to a QRsens code is given in Fig. 2a.

For the initial design of the code, any online QR code generator tool can be used (e.g., https://www.qrcode-monkey.com/). In this work, we propose two types of QRsens codes using two combinations of the five proposed sensors. Each combination is aimed at one particular application. In the first case, temperature, RH and $CO_2$ sensors are included in QRsens for enclosed spaces monitoring. The second combination includes $H_2S$, $NH_3$ and $CO_2$ sensors for smart packaging applications. According to the described design process, the first case will contain the following text encoded in the data area: *TEMP;$CO_2$;RH;URL*, while for the second case the encoded text will be: *$H_2S$;$CO_2$;$NH_3$;URL*. In both cases, for the fabrication of the different prototypes, the URL was chosen as the webpage of the research group for the proof-of-concept prototype. Following the same approach, other QRsens devices could be created by using different combinations of the colorimetric sensors, depending on the targeted application, and replacing the URL by any other custom information. The employed reagents and materials and the colorimetric inks fabrication process are described in Sections 1 and 2 of Supplementary Information (SI), respectively. Fig. 2b shows the fabrication process of the QRsens codes including the colorimetric inks deposition, which is described in more detail in Section 3 of SI.

### 2.2. Smartphone application development

A customized smartphone application was developed to simultaneously read the QR code and the colorimetric sensors. The programmed application implements automatic image processing for sensor detection and colour correction, data storage, and results sharing. Android Studio 4.2.2 was the integrated development environment (IDE) used to program the QRsens smartphone application. It was designed and tested against API 26 (Android 8.0). However, the application also supports previous Android versions, being API 18 (Android 4.3) the lowest API level compatible. The open-source computer vision OpenCV 3.1.0 Android library was employed for the acquisition and image processing tasks [32].

#### 2.2.1. Light colour correction

Practical usability of the developed QRsens smartphone application

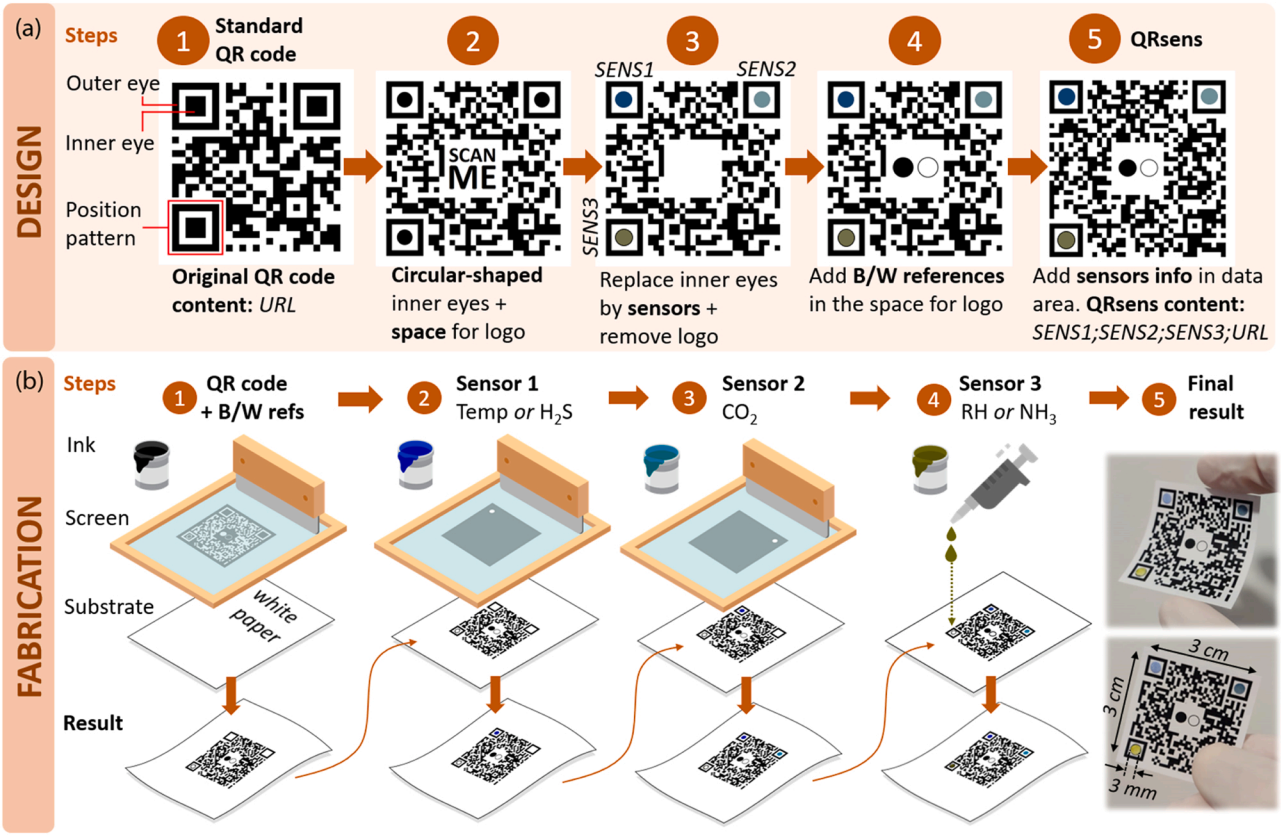


**Fig. 2.** **(a)** Design process from a standard original QR code to a QRsens code. **(b)** Fabrication steps of the QRsens code by screen printing and drop-casting. The final result photograph corresponds to the combination of temperature, RH and $CO_2$ sensors.

requires it to deliver consistent results independently of illumination changes. In many cases, this issue is mitigated through the attachment of external accessories to the smartphone to achieve controlled illumination conditions, such as opaque chambers to block ambient light, LEDs to provide constant illumination, and optical filters or lenses [33–35]. Software-based approaches have also been proposed to overcome this issue. One straightforward solution is to calibrate the system under different lighting conditions, storing several pre-loaded calibrations and fitting parameters within the application [36,37]. Another approach consists of using multiple colour reference markers corresponding to the colorimetric responses of the sensors obtained during the calibration phase [38–40]. The use of black and white reference markers is also a wider strategy that has yielded satisfactory results [41–44]. In some cases, colour space transformation has proven to be an effective method for quantitative colorimetric analysis robust to ambient lighting conditions, for instance using the hue–saturation–value (HSV) space [31]. Other authors have proposed more complex alternative algorithms to account for variations in ambient light [34,45,46]. Taking into account certain limitations depending on the specific case, all these software-based techniques enable the use of equipment-free imaging analysis, which is highly desirable for the end-user convenience.

In our case, we propose a two-step algorithm combining two of the previously described methods: a correction stage in the RGB colour space based on the B/W reference markers (printed in the centre of QRsens), followed by a colour space transformation to the HSV space. In this way, each acquired RGB colour coordinate of the sensors is adjusted with respect to each detected RGB value of the B/W references by:

$$RGB_{corrected} = 256 \cdot \frac{RGB_{sensor} - RGB_{black\_ref}}{RGB_{white\_ref}} \quad (1)$$

where RGB refers to the individual R, G or B colour coordinate of the sensor and reference in each case. The previous equation was applied in all cases except for the $H_2S$ sensor, in which a slightly different correction experimentally delivered better results:

$$RGB_{corrected} = 256 \cdot \frac{RGB_{sensor} - RGB_{black\_ref}}{RGB_{white\_ref} - RGB_{black\_ref}} \quad (2)$$

After the correction, the new RGB coordinates were converted to HSV values. In all cases, the normalised hue parameter ($H_{norm} = H/360$) was selected to quantify the sensor responses, except for the case of $CO_2$, where the saturation parameter (S) was chosen because it delivered a larger variation range or response (see Section 3.1). More details regarding the calibration setup and the measurement procedure are given in Section 4 of SI.

## 3. Results and discussion

### 3.1. QRsens application user flow

The accompanying Android application of QRsens consists of several screens that guide the user through the steps required for the acquisition and processing of a QRsens code. The whole process is depicted in the application user flow of Fig. 3a. Initially, there is a welcome screen that includes a menu with two options: *(1)* Scan QR code; and *(2)* Scan sensors. If the user chooses the first option, the application starts a QR reader screen so that the user can aim at the code with the smartphone camera to read its content, which is done in less than a second without needing to take any photograph. Upon detection and reading of the QRsens code, a pop-up window (alert dialog) with two options informs the user about the three sensors present in the device (which is encoded as part of the QRsens content), as well as the rest of the encoded custom information (e.g., an URL). In the fabricated proof-of-concept prototypes, an URL was embedded in the code, so at this point, the user can choose to directly visit that website (option 1 of the alert dialog) or scan the sensors (option 2). If the latter option is chosen, the application automatically starts the rear camera of the device so that the user can take a photograph of the QRsens code. To take the photograph, the developed app invokes through an intent to the free app Camera Zoom FX with the following set-up parameters: ISO 800, EV 0,0, auto focus and WB natural light. In principle, any external app could be called to take the photograph as long as the camera settings always remain constant. After this, the app allows the user to easily pinch to zoom in and out to fit the taken photograph of QRsens with the template grid (a white square superimposed on the screen), as shown in Fig. 3c. Once aligned, the user can slide the *Process* button to the right to start the automatic image processing, which is graphically summarised in Fig. 3b.

During the image processing conducted in the smartphone, the app only considers the region of interest (ROI) circumscribed by the white on-screen square, discarding the rest of the image to improve the consistency of the processing and eliminate the needless background. This masked image is then processed on the smartphone by means of the Circle Hough Transform (CHT) to detect the circle-shaped sensors and B/W references. CHT is a feature extraction technique used in digital image processing for detecting circular objects in imperfect digital image inputs, which our group has already employed in previous works [35]. In a similar way to such work, the image is converted to grayscale prior to the circle's detection using CHT, and also a Gaussian blur filter is applied to reduce the noise and avoid false detections. However, in this work, a significant improvement has been implemented in the processing pipeline, which consists of the application of a thresholding operation on the grayscale image (see Fig. 3b). After testing different thresholding methods, we concluded that the simplest technique (i.e., global binary thresholding) was the most suitable for our case. In binary thresholding, each pixel value is compared with a certain threshold value. If the pixel value is greater than the set threshold, that pixel is set to the maximum value (255); otherwise, it is set to 0 (black). Thresholding is a very popular segmentation technique with numerous applications in computer vision, and it is often used to separate objects considered as a foreground from its background (e.g., in text-recognition algorithms). We experimentally checked that this thresholding operation made the subsequent circle's detection algorithm much more reliable. After the binary thresholding and blurring operation, the Hough Transform function of OpenCV library was used to implement the circle detection in the QRsens code photograph. For each of the five circles detected by this algorithm (three corresponding to the sensors in the corners, and two corresponding to the B/W references), an individual mask is applied to eliminate everything from the image but the detected circle. In the creation of each mask, the radius of the circle is reduced by 20% to get away from the detected circle's edge. By doing so, we make sure that the colour of the sensor is detected completely inside the circle in case the edges are blurry. Upon the completion of the image processing, the app is able to provide information related to each detected circle, including its location (X-Y coordinates), size (radius), and average RGB and HSV colours. Based on the location information, the app automatically differentiates among the circles corresponding to the sensors and the B/W references. Subsequently, colour correction is applied using the B/W references to achieve a certain degree of environmental light independence (see Section 2.2.1). Afterwards, each sensor value is computed from the corresponding calibration curve, as previously described. When all the processing pipeline is finished, the app provides a report in plain text that is stored in the phone's memory, containing all the collected information about the QRsens code. The results (both image and report) can be shared through email and/or different messaging services through the *Share* button in the top menu of the application.

### 3.2. Light colour correction

Fig. 4 shows some examples of QRsens codes used during the calibration setup (see Section 4 in SI). In this case, one representative value of each sensor has been selected to show the effect of the light colour

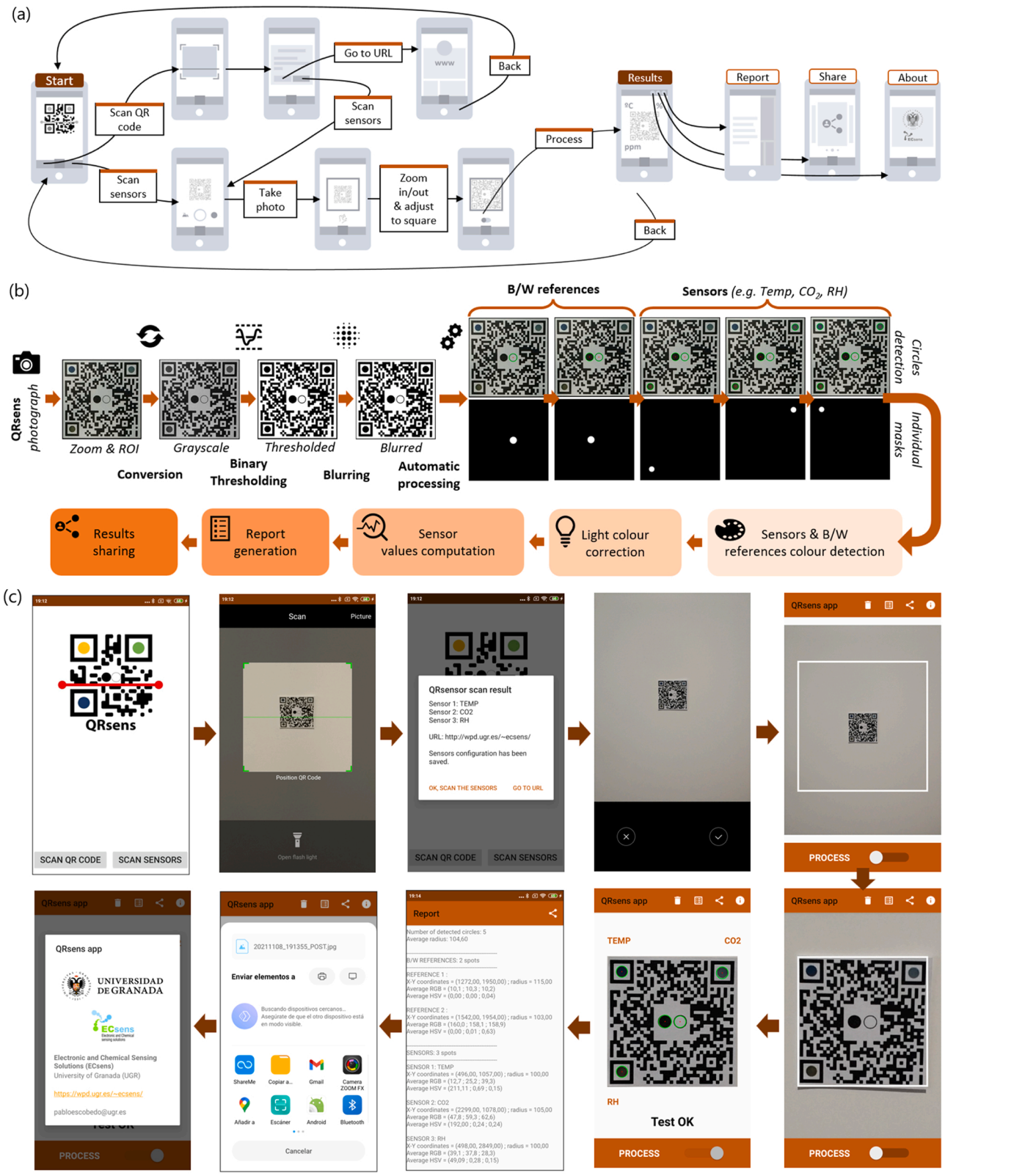


**Fig. 3.** **(a)** Application user flow showing the path that the user follows through the developed smartphone app interface to complete the acquisition of the QRsens device. **(b)** Flow diagram describing the image processing sequence conducted by the smartphone application. **(c)** Screen captures of the smartphone application corresponding to different steps of the described user flow.

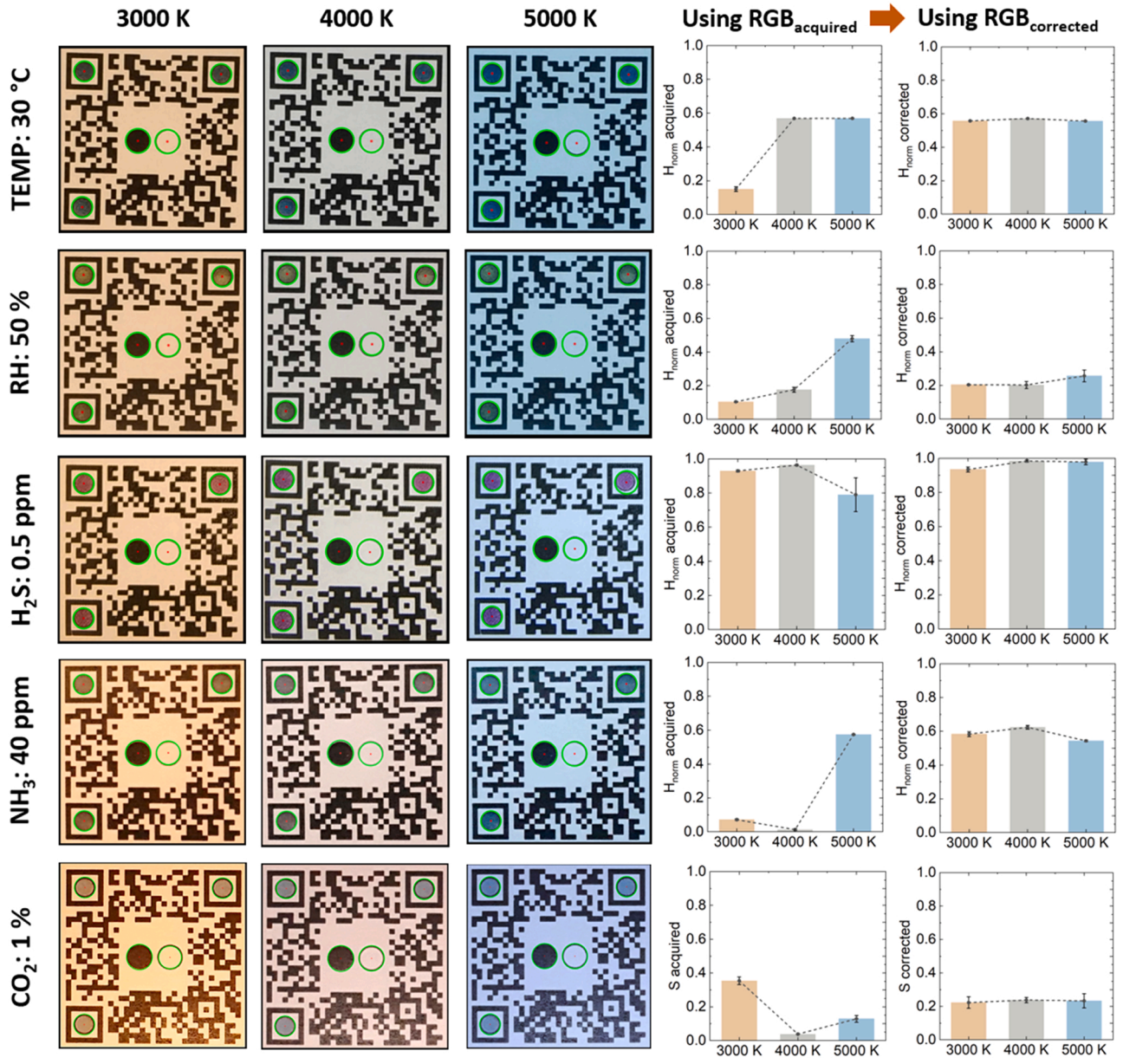


**Fig. 4.** Some representative examples of QRsens photographs for each sensor at particular values and different light colour temperatures (3000 K, 4000 K and 5000 K), comparing the acquired $H_{norm}$ parameter (for temperature, RH, $H_2S$ and $NH_3$ sensors) or S parameter (for the $CO_2$ sensor) before and after applying the light colour correction.

temperature correction. It can be observed how the computed values of $H_{norm}$ or S using the acquired RGB coordinates homogenise significantly after applying the light colour correction described in Section 2.2.1.

To provide a more accurate account of the achieved improvement, Table 1 quantifies this homogenization in terms of maximum standard deviation values ($SD_{max}$) for each sensor at the three considered light colour temperatures before and after applying the correction. In terms of $SD_{max}$, the obtained results show a minimum percentage decrease of ~71.4% and a maximum one of ~87%, which means a significant improvement and makes it possible to utilise QRsens under different illumination conditions. The chosen colour temperatures cover a wide range of potential real-life application scenarios of QRsens. For instance, warm white (3000 K) is typically used in general living spaces such as residences, hotels, restaurants, fruit and vegetable areas in supermarkets and commercial office spaces [47]. Neutral white (4000 K) is predominant in schools, office settings, hospitals, and shelf areas in supermarkets. Finally, 5000 K is similar to the midday sun, and it is best suited for places where high detail is required or where accurate colour rendering makes a difference on clothing, goods, or food. Some application scenarios would be warehouses, changing rooms, display areas, workshops, factories, manufacturing, and industrial facilities.

**Table 1**
Maximum standard deviation values for each sensor at the three considered light colour temperatures before and after applying the correction.

| Sensor | $SD_{max}$ before correction | $SD_{max}$ after correction | Percentage decrease (%) |
|---|---|---|---|
| Temperature | 0.28 | 0.04 | 85.71 |
| RH | 0.21 | 0.06 | 71.43 |
| $H_2S$ | 0.24 | 0.06 | 75.00 |
| $NH_3$ | 0.32 | 0.08 | 75.00 |
| $CO_2$ | 0.23 | 0.03 | 86.96 |

### 3.3. QRsens calibration and performance

Fig. 5 shows the performance curves obtained for the different sensors in QRsens, both under controlled illumination and after illumination correction. The exposure time for the tests was 2 min, time enough to prepare the standard analyte/nitrogen mixture and to reach the equilibrium (see Section 4 in SI). Typical fitting functions for this type of colorimetric sensors (i.e., Boltzmann sigmoidal and exponential functions) have been checked for each case, as shown in Fig. 5. Main analytical parameters of each sensor are shown in Table 2. The limits of detection (LODs) were obtained as 3 $s_b$ in case of exponential calibration function. When a sigmoidal shape response was obtained it was calculated by the tangent method as well as the upper limits [48]. The repeatability was quantified through the coefficient of variation (CV) of the signal, which is defined as the ratio between the standard deviation of a set of replicas and its mean value. An intermediate value in the range with the steeper slope was selected as representative for the CV calculation. The accuracies of the sensors considering the propagation of uncertainty (or propagation of error) of all parameters in the calibration functions have been also computed. Supplementary Table 1 shows the obtained results, which have been calculated using an intermediate point in the range with the steeper slope of each calibration curve as the representative value.

Regarding the calibration results shown in Fig. 5, it is worth noting that the error bars of the curves corresponding to the sensors after light colour correction are calculated as the standard deviations of the corrected parameters (either $H_{norm}$ or S) obtained after the corrections for the three colour temperatures. This is the reason why these error bars are significantly larger than the error bars for the cases where no light colour correction is conducted. Apart from this, it can also be observed

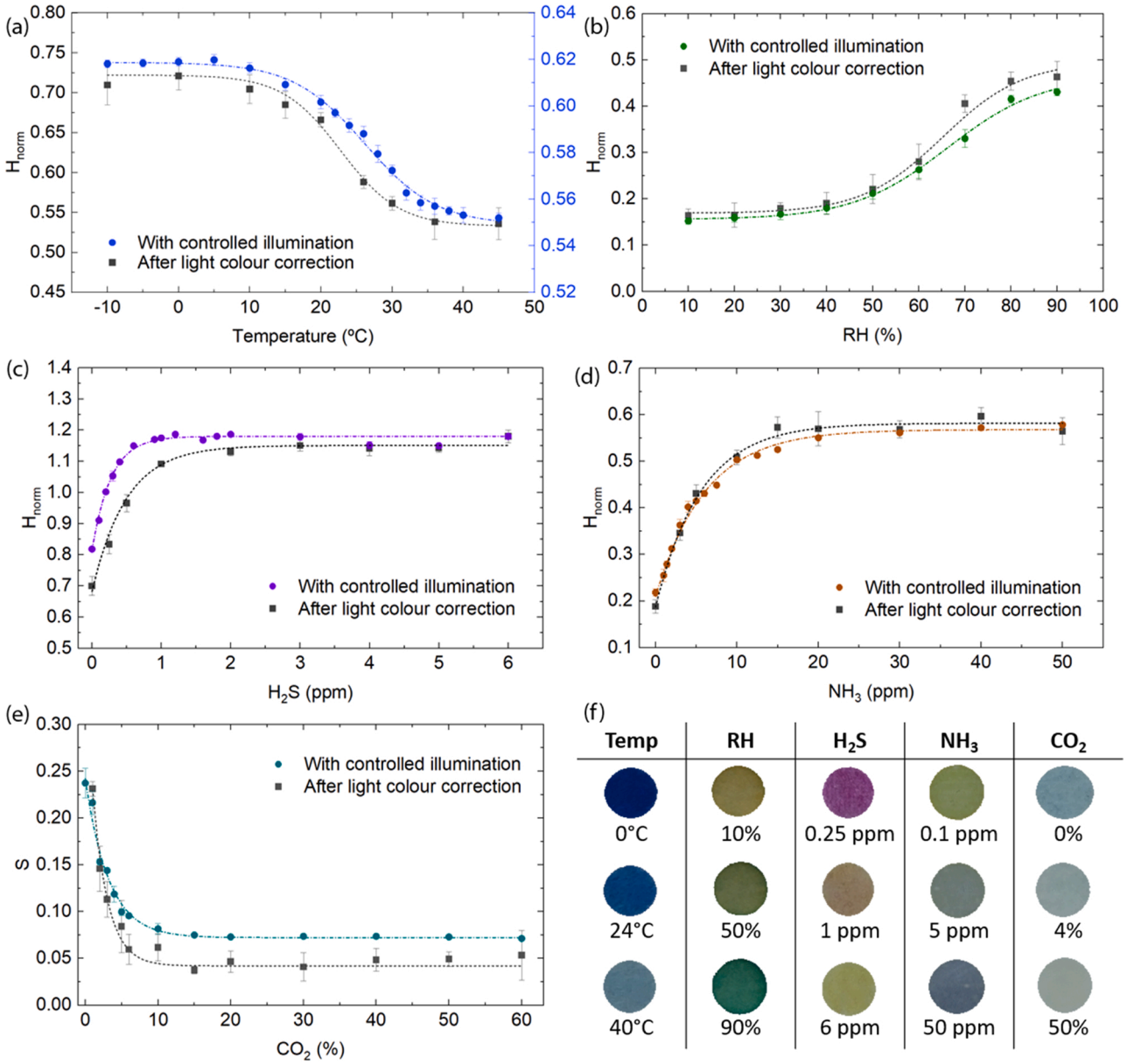


**Fig. 5.** Calibration curves of each sensor, both with controlled illumination and after illumination correction. The response of the **(a)** temperature, **(b)** RH, **(c)** $H_2S$ and **(d)** $NH_3$ are quantified by means of the normalised Hue parameter ($H_{norm}$), while the response of **(e)** $CO_2$ is quantified using the saturation (S) parameter. Fitting functions for each calibration curve and analytical parameters for each sensor are given in Table 1. Note that in the case of $H_2S$, from 1 ppm onwards it is necessary to add 1 unit to $H_{norm}$ to avoid the discontinuity. **(f)** Some examples of colour changes of different colorimetric sensors at several gas concentration/temperature/RH values.

**Table 2**
Calibration functions and analytical parameters of the colorimetric sensors with controlled illumination and after light colour correction.

| **Temperature sensor** | | | **RH sensor** | |
|---|---|---|---|---|
| Boltzmann function: | | | $y = \frac{A_1 - A_2}{1 + e^{\frac{x - A_3}{A_4}}} + A_2$ | |
| Parameter | With controlled illumination | After light colour correction | With controlled illumination | After light colour correction |
| $A_1$ | 0.6187 ± 0.0006 | 0.722 ± 0.006 | 0.156 ± 0.006 | 0.169 ± 0.005 |
| $A_2$ | 0.5490 ± 0.0015 | 0.533 ± 0.008 | 0.466 ± 0.019 | 0.497 ± 0.03 |
| $A_3$ | 26.2 ± 0.4 | 22.8 ± 0.9 | 66.3 ± 1.7 | 65 ± 3 |
| $A_4$ | 5.1 ± 0.3 | 4.1 ± 0.7 | 10.3 ± 1.4 | 8.8 ± 1.6 |
| $R^2$ | 0.99733 | 0.99102 | 0.9962 | 0.99521 |
| LOD | 14.9ºC | 13.4ºC | 44.6% | 46.7% |
| CV (%) | 0.56 (at 26ºC) | 1.38 (at 26ºC) | 7.1 (at 60%) | 13.7 (at 60%) |
| Detection range | 14.9–35.8ºC | 13.4–32.3ºC | 44.6–85.7% | 46.7–80.1% |
| **$H_2S$ sensor** | | | **$NH_3$ sensor** | |
| One-phase exponential growth function: | | | $y = A_1 e^{\frac{x}{A_3}} + A_2$ | |
| Parameter | With controlled illumination | After light colour correction | With controlled illumination | After light colour correction |
| $A_1$ | -0.37 ± 0.01 | -0.47 ± 0.03 | -0.358 ± 0.006 | -0.394 ± 0.011 |
| $A_2$ | 1.1802 ± 0.0023 | 1.151 ± 0.007 | 0.568 ± 0.003 | 0.582 ± 0.007 |
| $A_3$ | -0.273 ± 0.019 | -0.49 ± 0.04 | -6.13 ± 0.22 | -8.6 ± 0.4 |
| $R^2$ | 0.98934 | 0.98213 | 0.99494 | 0.99516 |
| LOD | 0.01 ppm | 0.13 ppm | 0.6 ppm | 0.7 ppm |
| CV (%) | 1.1 (at 0.5 ppm) | 2.8 (at 0.5 ppm) | 3.4 (at 3 ppm) | 4.6 (at 3 ppm) |
| Detection range | 0.01–0.6 ppm | 0.13–0.7 ppm | 0.6–7.7 ppm | 0.7–7.5 ppm |
| **$CO_2$ sensor** | | | | |
| One-phase exponential decay function: | | | $y = A_1 e^{\frac{-x}{A_3}} + A_2$ | |
| Parameter | | With controlled illumination | After light colour correction | |
| $A_1$ | | 0.170 ± 0.014 | 0.304 ± 0.024 | |
| $A_2$ | | 0.0723 ± 0.0007 | 0.042 ± 0.002 | |
| $A_3$ | | 3.2 ± 0.3 | 2.1 ± 0.3 | |
| $R^2$ | | 0.98702 | 0.99098 | |
| LOD | | 0.7% | 0.7% | |
| CV (%) | | 1.2 (at 3%) | 16.7 (at 3%) | |
| Detection range | | 0.7–5.2% | 0.7–4.1% | |

in Table 2 that the performance of QRsens codes is better for the cases where illumination conditions are controlled, in terms of lower LODs and CVs and wider ranges, as would be expected.

However, in practice, illumination colour correction will be required in most cases. As shown in Table 2, after light colour correction the colorimetric gas sensors exhibit a detection range of 0.7–4.1%, 0.7–7.5 ppm, and 0.13–0.7 ppm for $CO_2$, $NH_3$ and $H_2S$, respectively. In the case of temperature and RH, the detection ranges are 13.4–32.3ºC and 46.7–80.1%, respectively. The temperature detection range could be extended by using another commercial thermochromic ink different to the one used that exhibits an alternative detectable temperature window. On the other hand, we can observe in the case of light colour correction in Fig. 5a,b,e higher slopes in the non-saturation region, which means an increase of sensitivity of temperature, RH and $CO_2$ sensors. These slope increases resulted in decreased ranges due to the constancy of the difference of the saturation values. Therefore, the potential application scenario of QRsens will determine all these analytical parameters as well as the expected accuracy of the system. For instance, if QRsens is applied in a place where lightning conditions remain unchanged and controlled (e.g., display cabinet, supermarket, office, etc.), it will allow lower LODs and larger ranges with better repeatability and accuracy. Otherwise, if illumination conditions dynamically change and cannot be controlled, QRsens will still be usable, thanks to the implemented automatic light colour correction, although with a slightly lower performance. In some cases, the obtained dynamic ranges of the colorimetric sensors (Table 2) will also influence the potential application scenarios of QRsens. The most restrictive case is obtained for the $CO_2$ sensor, which could be used in QRsens as a threshold detector to generate an alarm rather than a quantitative indicator. For instance, for smart packaging applications QRsens could inform of a leakage in the package, since $CO_2$ is typically flushed into the package to obtain concentrations above 60%. For enclosed space monitoring, QRsens could serve as a threshold alarm if $CO_2$ largely exceeds the health safety limits.

To study the cross-sensitivity among the sensors, the maximum variation of the output signal of the sensors in the presence of the rest of the gases was obtained for a fixed concentration of the target gas. The influence of the temperature was also quantified as the variation of the output signal to an increment of 25 °C. The obtained results are shown in Supplementary Table 2 of SI. Data measured for this work and those taken from the literature have shown that, in a practical case, the cross-sensitivity can be neglected [22,49]. The interference produced by the gases in response to the other gases sensors is below 3%, presenting the maximum deviation when the interfering gas is present in a very high concentration, which is not a realistic case. This implies that in a practical case the cross-sensitivity can be neglected. There is only one exception to this fact: the influence of $NH_3$ on the response of the humidity sensor, with a maximum variation above 21%. Therefore, in the case of $NH_3$ in high concentrations, humidity sensor output should be corrected. A linear relationship was experimentally found between the output signal of RH with the increase of $NH_3$, whose details are given in Section 5 of SI. Thus, in potential applications where presence of $NH_3$ in high concentrations is expected, the RH sensor output can be corrected based on such relationship.

It is worth mentioning that in the same context as QRsens, several interesting developments of QR-like codes with colorimetric sensing can be found in the literature, which have been compiled and summarised in Table 3. In comparison with other approaches, our solution proposes five different sensors (that can be combined into groups of three sensors), which have never been simultaneously combined in previous solutions, thus opening new potential applications.

### 3.4. Conclusions

To sum up, a fully functional QR code has been enhanced with built-in multi-sensing functionality (QRsens) for in situ environment analysis. Our system distinguishes from state-of-the-art solutions by combining the following aspects simultaneously: Firstly, QRsens codes are still valid for their original purpose as information storage devices, being the sensing functionality an add-on feature that does not undermine the usefulness of the original QR code. Secondly, to provide fast and quantitative readings, a user-friendly smartphone application was programmed for image processing, data storage, and/or sharing. Thirdly, a light colour correction solution is seamlessly integrated into the code to make the system viable under different lighting conditions. Lastly, the use of a standard fabrication technique (screen-printing) and flexible substrate (paper) opens up the possibility to produce QRsens codes by establishing high-volume manufacturing methods such as roll-to-roll printing.

## Declaration of Competing Interest

The authors declare that they have no known competing financial interests or personal relationships that could have appeared to influence the work reported in this paper.

**Table 3**
Examples of QR-like codes with colorimetric sensors found in the literature.

| Sensor (s) | Substrate | Fabrication technology | Light colour correction? | QR valid for data storage? | Smartphone app developed? | Ref |
|---|---|---|---|---|---|---|
| Temperature | Plastic (acetate) | Non-standard | No | Yes | Yes | [50] |
| 12 chemoresponsive dyes for olive oil odour id. | Paper | Wax printing | No | No | No | [51] |
| $NH_3$ | Plastic (acetate/ polyester) | Inkjet and screen printing | Yes | No | No | [52] |
| $NH_3$, $CH_2O$ and $H_2S$ | Paper/plastic | Screen printing | Yes | No | No | [53] |
| Enzyme-linked antibodies | Paper | Laser Induced Forward Transfer | No | No | No | [54] |
| $Cu^{2+}$ (semiquantitative) | Paper | Solid ink and inkjet printing | Yes | Yes | No | [55] |
| Escherichia coli | Paper | Wax printing + Deposition | No | Yes | No | [56] |
| Temperature | Paper | Inkjet printing | No | Yes | No | [57] |
| RH | Photonic crystal (PC) film | Spin coating | No | Yes | No | [58] |
| Protein | Paper | Wax printing | No | Yes | No | [59] |
| pH | Paper | Inkjet printing | No | Yes | No | [60] |
| Histidine-rich protein II (malarial biomarker) | Nitrocellulose membrane | Non-standard | Yes | Yes | Yes | [61] |
| Cholesterol | Paper | Wax printing | No | Yes | No | [62] |
| Temperature, RH, $CO_2$, $NH_3$ and $H_2S$ | Paper | Screen printing | Yes | Yes | Yes | This work |

## Data Availability

Data will be made available on request.

## Acknowledgements

This study was funded by Spanish MCIN/AEI/10.13039/501100011033/ (Projects PID2019–103938RB-I00, ECQ2018–004937-P and grant IJC2020–043307-I) and Junta de Andalucía (Projects B-FQM-243-UGR18, P18-RT-2961). The projects and the grant were partially supported by European Regional Development Funds (ERDF) and by European Union NextGenerationEU/PRTR.

### *CRediT authorship contribution statement*

**Pablo Escobedo:** Conceptualization, Methodology, Software, Validation, Investigation, Formal analysis, Writing – original draft, Visualisation, Supervision. **Celia E. Ramos-Lorente:** Methodology, Investigation, Formal analysis, Writing – original draft. **Ammara Ejaz:** Conceptualization, Formal analysis, Writing – review & editing. **Miguel M. Erenas:** Methodology, Validation, Investigation, Formal analysis, Writing – original draft. **Antonio Martínez-Olmos:** Methodology, Investigation, Formal analysis. **Miguel A. Carvajal:** Methodology, Investigation, Formal analysis. **Carlos García-Núñez:** Formal analysis, Writing – review & editing, Supervision. **Ignacio de Orbe-Payá:** Formal analysis, Writing – review & editing. **Luis F. Capitán-Vallvey:** Methodology, Investigation, Writing – original draft, Supervision, Project administration. **Alberto J. Palma:** Methodology, Investigation, Writing – original draft, Supervision, Project administration. All authors have read and agreed to the published version of the manuscript.

## Appendix A. Supporting information

Supplementary data associated with this article can be found in the online version at doi:10.1016/j.snb.2022.133001.

## References

[1] M. Vazquez-Briseno, F.I. Hirata, J. de, D. Sanchez-Lopez, E. Jimenez-Garcia, C. Navarro-Cota, J.I. Nieto-Hipolito, Using RFID/NFC and QR-Code in Mobile Phones to Link the Physical and the Digital World, IntechOpen, 2012, https://doi.org/10.5772/37447.

[2] C. Aktaş, The Evolution and Emergence of QR Codes, Cambridge Scholars Publishing, 2017.

[3] C. Law, S. So, QR codes in education, JETDE 3 (2010), https://doi.org/10.18785/jetde.0301.07.

[4] N. Min-Allah, B.A. Alahmed, E.M. Albreek, L.S. Alghamdi, D.A. Alawad, A. S. Alharbi, N. Al-Akkas, D. Musleh, S. Alrashed, A survey of COVID-19 contact-tracing apps, Comput. Biol. Med. 137 (2021), 104787, https://doi.org/10.1016/j.compbiomed.2021.104787.

[5] A.W. Colman, J.F.K. Sellick, J.U. Weaver, Use of Quick Response (QR) coded bracelets and cards for the improvement of cortisol deficiency/Addison's disease management: an audit of quality of care of the management of steroid deficiency in acute illness, BMJ Innov. 4 (2018), https://doi.org/10.1136/bmjinnov-2017-000226.

[6] M. Vázquez-Briseño, J. Nieto-Hipólito, E. Jiménez-García, Using QR Codes to Improve Mobile Wellness Applications, Undefined. (2010). ⟨https://www.semanticscholar.org/paper/Using-QR-Codes-to-Improve-Mobile-Wellness-V%C3%A1zquez-Brise%C3%B1o-Nieto-Hip%C3%B3lito/dfbc26b901801fd0f881b55b1b3dff4101c0cbc6⟩ (accessed November 18, 2021).

[7] J. Sanz-Valero, L.M. Álvarez Sabucedo, C. Wanden-Berghe, J.M. Santos Gago, QR codes: outlook for food science and nutrition, Crit. Rev. Food Sci. Nutr. 56 (2016) 973–978, https://doi.org/10.1080/10408398.2012.742865.

[8] R. Barthel, A. Hudson-smith, M.D. Jode, B. Blundell, Tales of Things The Internet of 'Old ' Things: Collecting Stories of Objects, Places and Spaces, (n.d.).

[9] A. Hudson-Smith, S. Gray, C. Ross, R. Barthel, M. de Jode, C. Warwick, M. Terras, Experiments with the internet of things in museum space: QRator. Proceedings of the 2012 ACM Conference on Ubiquitous Computing, Association for Computing Machinery, New York, NY, USA, 2012, pp. 1183–1184, https://doi.org/10.1145/2370216.2370469.

[10] J.Z. Gao, L. Prakash, R. Jagatesan, Understanding 2D-BarCode Technology and Applications in M-Commerce - Design and Implementation of A 2D Barcode Processing Solution, in: 31st Annual International Computer Software and Applications Conference (COMPSAC 2007), 2007: pp. 49–56. ⟨https://doi.org/10.1109/COMPSAC.2007.229⟩.

[11] I. Tkachenko, W. Puech, C. Destruel, O. Strauss, J.-M. Gaudin, C. Guichard, Two-level QR code for private message sharing and document authentication, IEEE Trans. Inf. Forensics Secur. 11 (2016) 571–583, https://doi.org/10.1109/TIFS.2015.2506546.

[12] H. Li, T. Chen, Y. Peng, H. Li, An intelligent vehicle-tracking system solution for indoor parking, Appl. Geomat. 12 (2020) 481–490, https://doi.org/10.1007/s12518-020-00321-8.

[13] A. Luvisi, Electronic identification technology for agriculture, plant, and food. A review, Agron. Sustain. Dev. 36 (2016) 1–14, https://doi.org/10.1007/s13593-016-0352-3.

[14] C.T. Karia, A. Hughes, S. Carr, Uses of quick response codes in healthcare education: a scoping review, BMC Med Educ. 19 (2019) 456, https://doi.org/10.1186/s12909-019-1876-4.

[15] T.M. Fernández-Caramés, P. Fraga-Lamas, A review on human-centered IoT-connected smart labels for the industry 4.0, IEEE Access 6 (2018) 25939–25957, https://doi.org/10.1109/ACCESS.2018.2833501.

[16] H. El Matbouly, P. Escobedo, R. Dahiya, Flexible Metasurface QR Code for Simultaneous Identification and Sensing, in: 2021 IEEE International Conference on Flexible and Printable Sensors and Systems (FLEPS), 2021: pp. 1–4. https://doi.org/10.1109/FLEPS51544.2021.9469817.

[17] N. Tang, C. Zhou, L. Xu, Y. Jiang, H. Qu, X. Duan, A fully integrated wireless flexible ammonia sensor fabricated by soft nano-lithography, ACS Sens. 4 (2019) 726–732, https://doi.org/10.1021/acssensors.8b01690.
[18] S. Matindoust, A. Farzi, M. Baghaei Nejad, M.H. Shahrokh Abadi, Z. Zou, L. R. Zheng, Ammonia gas sensor based on flexible polyaniline films for rapid detection of spoilage in protein-rich foods, J. Mater. Sci.: Mater. Electron. 28 (2017) 7760–7768, https://doi.org/10.1007/s10854-017-6471-z.
[19] X. Zhai, Z. Li, J. Shi, X. Huang, Z. Sun, D. Zhang, X. Zou, Y. Sun, J. Zhang, M. Holmes, Y. Gong, M. Povey, S. Wang, A colorimetric hydrogen sulfide sensor based on gellan gum-silver nanoparticles bionanocomposite for monitoring of meat spoilage in intelligent packaging, Food Chem. 290 (2019) 135–143, https://doi.org/10.1016/j.foodchem.2019.03.138.
[20] J. Koskela, J. Sarfraz, P. Ihalainen, A. Määttänen, P. Pulkkinen, H. Tenhu, T. Nieminen, A. Kilpelä, J. Peltonen, Monitoring the quality of raw poultry by detecting hydrogen sulfide with printed sensors, Sens. Actuators B: Chem. 218 (2015) 89–96, https://doi.org/10.1016/j.snb.2015.04.093.
[21] P. Puligundla, J. Jung, S. Ko, Carbon dioxide sensors for intelligent food packaging applications, Food Control 25 (2012) 328–333, https://doi.org/10.1016/j.foodcont.2011.10.043.
[22] P. Escobedo, M.M. Erenas, N. López-Ruiz, M.A. Carvajal, S. Gonzalez-Chocano, I. de Orbe-Payá, L.F. Capitán-Valley, A.J. Palma, A. Martínez-Olmos, Flexible passive near field communication tag for multigas sensing, Anal. Chem. 89 (2017) 1697–1703, https://doi.org/10.1021/acs.analchem.6b03901.
[23] K. Azuma, N. Kagi, U. Yanagi, H. Osawa, Effects of low-level inhalation exposure to carbon dioxide in indoor environments: a short review on human health and psychomotor performance, Environ. Int. 121 (2018) 51–56, https://doi.org/10.1016/j.envint.2018.08.059.
[24] P. Escobedo, M.D. Fernández-Ramos, N. López-Ruiz, O. Moyano-Rodríguez, A. Martínez-Olmos, I.M. Pérez de Vargas-Sansalvador, M.A. Carvajal, L.F. Capitán-Vallvey, A.J. Palma, Smart facemask for wireless $CO_2$ monitoring, Nat. Commun. 13 (2022) 72, https://doi.org/10.1038/s41467-021-27733-3.
[25] M. Frankel, G. Bekö, M. Timm, S. Gustavsen, E.W. Hansen, A.M. Madsen, Seasonal variations of indoor microbial exposures and their relation to temperature, relative humidity, and air exchange rate, Appl. Environ. Microbiol. 78 (2012) 8289–8297, https://doi.org/10.1128/AEM.02069-12.
[26] A. Aganovic, Y. Bi, G. Cao, F. Drangsholt, J. Kurnitski, P. Wargocki, Estimating the impact of indoor relative humidity on SARS-CoV-2 airborne transmission risk using a new modification of the Wells-Riley model, Build. Environ. 205 (2021), 108278, https://doi.org/10.1016/j.buildenv.2021.108278.
[27] Z. Peng, J.L. Jimenez, Exhaled $CO_2$ as a COVID-19 infection risk proxy for different indoor environments and activities, Environ. Sci. Technol. Lett. 8 (2021) 392–397, https://doi.org/10.1021/acs.estlett.1c00183.
[28] M.M. Hassan, M.E. El Zowalaty, S.A. Khan, A. Islam, Md.R.K. Nayem, J.D. Järhult, Role of environmental temperature on the attack rate and case fatality rate of coronavirus disease 2019 (COVID-19) pandemic, Infect. Ecol. Epidemiol. 10 (2020) 1792620, https://doi.org/10.1080/20008686.2020.1792620.
[29] C. Rolfe, H. Daryaei, Intrinsic and extrinsic factors affecting microbial growth in food systems, in: A. Demirci, H. Feng, K. Krishnamurthy (Eds.), Food Safety Engineering, Springer International Publishing, Cham, 2020, pp. 3–24, https://doi.org/10.1007/978-3-030-42660-6_1.
[30] J. Lelieveld, J.S. Evans, M. Fnais, D. Giannadaki, A. Pozzer, The contribution of outdoor air pollution sources to premature mortality on a global scale, Nature 525 (2015) 367–371, https://doi.org/10.1038/nature15371.
[31] Safety and Health Topics | Hydrogen Sulfide - Hazards | Occupational Safety and Health Administration, (2020). ⟨https://www.osha.gov/hydrogen-sulfide⟩ (accessed November 18, 2021).
[32] G. Bradski, A. Kaehler, Learning OpenCV: Computer Vision with the OpenCV Library, O'Reilly Media, Inc, 2008.
[33] S.C. Kim, U.M. Jalal, S.B. Im, S. Ko, J.S. Shim, A smartphone-based optical platform for colorimetric analysis of microfluidic device, Sens. Actuators B: Chem. 239 (2017) 52–59, https://doi.org/10.1016/j.snb.2016.07.159.
[34] V. Oncescu, D. O'Dell, D. Erickson, Smartphone based health accessory for colorimetric detection of biomarkers in sweat and saliva, Lab Chip 13 (2013) 3232–3238, https://doi.org/10.1039/c3lc50431j.
[35] P. Escobedo, M.M. Erenas, A. Martinez Olmos, M.A. Carvajal, M. Tabraue Chavez, M.A. Luque Gonzalez, J.J. Diaz-Mochon, S. Pernagallo, L.F. Capitan-Vallvey, A. J. Palma, Smartphone-based diagnosis of parasitic infections with colorimetric assays in centrifuge tubes, IEEE Access 7 (2019) 185677–185686, https://doi.org/10.1109/ACCESS.2019.2961230.
[36] T. Alawsi, G.P. Mattia, Z. Al-Bawi, R. Beraldi, Smartphone-based colorimetric sensor application for measuring biochemical material concentration, Sens. Bio-Sens. Res. 32 (2021), 100404, https://doi.org/10.1016/j.sbsr.2021.100404.
[37] A.K. Yetisen, J.L. Martinez-Hurtado, A. Garcia-Melendrez, F. da Cruz Vasconcellos, C.R. Lowe, A smartphone algorithm with inter-phone repeatability for the analysis of colorimetric tests, Sens. Actuators B: Chem. 196 (2014) 156–160, https://doi.org/10.1016/j.snb.2014.01.077.
[38] J. Choi, A.J. Bandodkar, J.T. Reeder, T.R. Ray, A. Turnquist, S.B. Kim, N. Nyberg, A. Hourlier-Fargette, J.B. Model, A.J. Aranyosi, S. Xu, R. Ghaffari, J.A. Rogers, Soft, skin-integrated multifunctional microfluidic systems for accurate colorimetric analysis of sweat biomarkers and temperature, ACS Sens 4 (2019) 379–388, https://doi.org/10.1021/acssensors.8b01218.
[39] M.E. Ferreira, J. Tirapu-Azpiroz, D.V.L.M. Marçal, A.F. da Silva, R.L. Ohta, M. B. Steiner, Illumination compensation algorithm for colorimetric detection of microfluidic paper-based devices with a smartphone. Optical Diagnostics and Sensing XXI: Toward Point-of-Care Diagnostics, SPIE,, 2021, pp. 15–25, https://doi.org/10.1117/12.2578441.
[40] H. Karlsen, T. Dong, Smartphone-based rapid screening of urinary biomarkers, IEEE Trans. Biomed. Circuits Syst. 11 (2017) 455–463, https://doi.org/10.1109/TBCAS.2016.2633508.
[41] J.I. Hong, B.-Y. Chang, Development of the smartphone-based colorimetry for multi-analyte sensing arrays, Lab Chip 14 (2014) 1725–1732, https://doi.org/10.1039/c3lc51451j.
[42] M.-Y. Jia, Q.-S. Wu, H. Li, Y. Zhang, Y.-F. Guan, L. Feng, The calibration of cellphone camera-based colorimetric sensor array and its application in the determination of glucose in urine, Biosens. Bioelectron. 74 (2015) 1029–1037, https://doi.org/10.1016/j.bios.2015.07.072.
[43] A. Koh, D. Kang, Y. Xue, S. Lee, R.M. Pielak, J. Kim, T. Hwang, S. Min, A. Banks, P. Bastien, M.C. Manco, L. Wang, K.R. Ammann, K.I. Jang, P. Won, S. Han, R. Ghaffari, U. Paik, M.J. Slepian, G. Balooch, Y. Huang, J.A. Rogers, A soft, wearable microfluidic device for the capture, storage, and colorimetric sensing of sweat, Sci. Transl. Med. 8 (2016), https://doi.org/10.1126/scitranslmed.aaf2593.
[44] T. Kong, J.B. You, B. Zhang, B. Nguyen, F. Tarlan, K. Jarvi, D. Sinton, Accessory-free quantitative smartphone imaging of colorimetric paper-based assays, Lab Chip 19 (2019) 1991–1999, https://doi.org/10.1039/C9LC00165D.
[45] M. Nixon, F. Outlaw, T.S. Leung, Accurate device-independent colorimetric measurements using smartphones, PLoS ONE 15 (2020), e0230561, https://doi.org/10.1371/journal.pone.0230561.
[46] X. Bao, S. Jiang, Y. Wang, M. Yu, J. Han, A remote computing based point-of-care colorimetric detection system with a smartphone under complex ambient light conditions, Analyst 143 (2018) 1387–1395, https://doi.org/10.1039/C7AN01685A.
[47] M. Karlen, C. Spangler, J.R. Benya, Lighting Design Basics, John Wiley & Sons, 2017.
[48] G. Mistlberger, G.A. Crespo, E. Bakker, Ionophore-based optical sensors, Annu. Rev. Anal. Chem. 7 (2014) 483–512, https://doi.org/10.1146/annurev-anchem-071213-020307.
[49] M. Ariza-Avidad, M. Agudo-Acemel, A. Salinas-Castillo, L.F. Capitán-Vallvey, Inkjet-printed disposable metal complexing indicator-displacement assay for sulphide determination in water, Anal. Chim. Acta 872 (2015) 55–62, https://doi.org/10.1016/j.aca.2015.02.045.
[50] J.F.C.B. Ramalho, S.F.H. Correia, L. Fu, L.L.F. António, C.D.S. Brites, P.S. André, R. A.S. Ferreira, L.D. Carlos, Luminescence thermometry on the route of the mobile-based internet of things (IoT): how smart QR codes make it real, Adv. Sci. 6 (2019) 1900950, https://doi.org/10.1002/advs.201900950.
[51] J.A.M. Conrado, R. Sequinel, B.C. Dias, M. Silvestre, A.D. Batista, J.F. da S. Petruci, Chemical QR code: a simple and disposable paper-based optoelectronic nose for the identification of olive oil odor, Food Chem. 350 (2021), 129243, https://doi.org/10.1016/j.foodchem.2021.129243.
[52] I. Benito-Altamirano, P. Pfeiffer, O. Cusola, J. Daniel Prades, Machine-readable pattern for colorimetric sensor interrogation, Proceedings 2 (2018) 906, https://doi.org/10.3390/proceedings2130906.
[53] L. Engel, I. Benito-Altamirano, K.R. Tarantik, C. Pannek, M. Dold, J.D. Prades, J. Wöllenstein, Printed sensor labels for colorimetric detection of ammonia, formaldehyde and hydrogen sulfide from the ambient air, Sens. Actuators B: Chem. 330 (2021), 129281, https://doi.org/10.1016/j.snb.2020.129281.
[54] I.N. Katis, J.A. Holloway, J. Madsen, S.N. Faust, S.D. Garbis, P.J.S. Smith, D. Voegeli, D.L. Bader, R.W. Eason, C.L. Sones, Paper-based colorimetric enzyme linked immunosorbent assay fabricated by laser induced forward transfer, Biomicrofluidics 8 (2014), 036502, https://doi.org/10.1063/1.4878696.
[55] A. Katoh, K. Maejima, Y. Hiruta, D. Citterio, All-printed semiquantitative paper-based analytical devices relying on QR code array readout, Analyst 145 (2020) 6071–6078, https://doi.org/10.1039/D0AN00955E.
[56] A. Burklund, H.K. Saturley-Hall, F.A. Franchina, J.E. Hill, J.X.J. Zhang, Printable QR code paper microfluidic colorimetric assay for screening volatile biomarkers, Biosens. Bioelectron. 128 (2019) 97–103, https://doi.org/10.1016/j.bios.2018.12.026.
[57] B. Yoon, H. Shin, E.-M. Kang, D.W. Cho, K. Shin, H. Chung, C.W. Lee, J.-M. Kim, Inkjet-compatible single-component polydiacetylene precursors for thermochromic paper sensors, ACS Appl. Mater. Interfaces 5 (2013) 4527–4535, https://doi.org/10.1021/am303300g.
[58] D. Kou, W. Ma, S. Zhang, J.L. Lutkenhaus, B. Tang, High-performance and multifunctional colorimetric humidity sensors based on mesoporous photonic crystals and nanogels, ACS Appl. Mater. Interfaces 10 (2018) 41645–41654, https://doi.org/10.1021/acsami.8b14223.
[59] H. Hall, A. Syed, J.X.J. Zhang, Two-dimensional, error-corrected barcode readout for point-of-care colorimetric assays, in: 2016 IEEE Healthcare Innovation Point-Of-Care Technologies Conference (HI-POCT), 2016: pp. 81–84. ⟨https://doi.org/10.1109/HIC.2016.7797702⟩.
[60] Y. Xu, Z. Liu, R. Liu, M. Luo, Q. Wang, L. Cao, S. Ye, Inkjet-printed pH-sensitive QR code labels for real-time food freshness monitoring, J. Mater. Sci. 56 (2021) 18453–18462, https://doi.org/10.1007/s10853-021-06477-x.
[61] T.F. Scherr, S. Gupta, D.W. Wright, F.R. Haselton, An embedded barcode for "connected" malaria rapid diagnostic tests, Lab Chip 17 (2017) 1314–1322, https://doi.org/10.1039/c6lc01580h.
[62] T. Wang, G. Xu, W. Wu, X. Wang, X. Chen, S. Zhou, F. You, A novel combination of quick response code and microfluidic paper-based analytical devices for rapid and quantitative detection, Biomed. Microdevices 20 (2018) 79, https://doi.org/10.1007/s10544-018-0325-1.

**Pablo Escobedo** received the Major degrees in Telecommunication Engineering and Electronics Engineering from the University of Granada (Granada, Spain) in 2012 and 2013, respectively, and the M.Sc. degree in Computer and Network Engineering in 2014.

In 2018, he completed his PhD at the University of Granada, focused on the design and development of printed sensor systems on flexible substrates, with special interest in RFID/NFC technology with sensing capabilities. After a postdoctoral stage at University of Glasgow (Scotland, United Kingdom), since 2021 he is postdoctoral research fellow in the ECSens group (Electronic and Chemical sensing solutions) at University of Granada. His research includes the development of printed smart labels and sensing systems for environmental, health, sport, and food quality monitoring applications.

**Celia E. Ramos-Lorente** received her degree in chemistry at the University of Granada in 2019. She is currently finishing a combination of two master's programs in Teaching Training in Obligatory Secondary and Upper Secondary School Education, Vocational Training and Languages and in Chemical Sciences and Technologies at the Official Postgraduate School in the same university. She is interested in colorimetric microfluidic thread and cloth-based sensors.

**Ammara Ejaz** obtained her PhD in Electroanalytical Chemistry from Chonnam National University (CNU), South Korea (Sep 2014 – Feb 2019). Dr. Ejaz's PhD dissertation was primarily focused on an insightful in-situ study about the growth kinetics of nanoparticles from the individual influence of pyrrolic, pyridinic, graphitic–N, and solvents. Besides, she thoroughly studied the structure-reactivity correlation of nanoparticles-based catalysts for the Fuel cell, Electrochemical, and Biosensors. She was a Research Professor at the Department of Chemical Engineering (Sep 2018 – Sep 2019), CNU, and later went on joining as a Research Assistant at the School of Engineering, the University of Glasgow (Sep 2018 – Sep 2021) to work on pre/post functionalization of electrospun fibers with nanoparticles by exploiting covalent, electrostatic, and π - π stacking interactions for food quality monitoring by embedding colorimetric sensors on the packaging. Currently, Dr. Ejaz is working at the Institute of thin films, sensors and imaging at the University of West of Scotland, Glasgow, to engineer energy harvesting systems and their miniaturized integration with supercapacitors for self-power electronics and their subsequent commercialization.

**Miguel M. Erenas** received the MSc degree (2004) and the PhD degree in Analytical Chemistry (2011) from the University of Granada (Granada, Spain). He is Assistant Professor at the Department of Analytical Chemistry, University of Granada. His research interests include the use of imaging along with microfluidic disposable sensors based on thread and paper for bioanalysis and food quality analysis.

**Antonio Martínez-Olmos** was born in 1980 in Granada (Spain). He received the M.Sc. degree and the PhD degree in Electronic Engineering from the University of Granada (Granada, Spain) in 2003 and 2009, respectively. Currently he works as an Associate Professor at the University of Granada. His current research includes the design of tomography sensors and the study of optical sensors for different biological measurements.

**Miguel A. Carvajal** was born in 1977 in Granada (Spain). He received the MSc degrees in Physics in 2000 and the MSc degree in Electronic Engineering in 2002, both from the University of Granada; and the PhD degree in Electronic Engineering from the University of Granada in 2007 about the development a dosimeter system based on commercial MOSFETs. Currently he works as tenured Professor at the University of Granada. His research interests include the effects of irradiation and post-irradiation in MOSFET transistors, RFID tags with sensor capabilities, gas sensor and electrochemiluminescent sensors, and their applications to handheld instrumentation.

**Carlos García Núñez**, Lecturer in Physics in the University of the West of Scotland, received his B.S. degree in Physics in 2009, his M.S. degree in Advanced Materials and Nanotechnology in 2010, and his PhD degree in Physics in 2015 at the Universidad Autónoma de Madrid (Spain). Dr. García Núñez's PhD dissertation was primarily focused on the synthesis of semiconductor nanowires using chemical beam epitaxy and chemical vapour transport techniques and their integration in IR/VIS/UV photodetectors through dielectrophoresis. From 2015–2018, he was Postdoctoral Researcher at the University of Glasgow (UK) developing wearable optoelectronics and sensors based on semiconductor nanowires and graphene. He is author in presentations and publications (95), with a h-index of 21, accumulating more than 1733 citations since 2012. He has published up to 44 journal papers (18 as first author) in high IF journals, and 15 conference proceedings, 2 books, and 2 intellectual properties. His research interest includes synthesis and characterization of semiconductor materials with the shape of nanowires and thin films, and 2D materials, for the development of optoelectronics, sensors, and energy systems.

**Ignacio de Orbe Payá** is Associate Professor of the Department of Analytical Chemistry at the University of Granada (Spain). His main areas of research are the development of the sensing phases for their use as chemical sensors in the determination of inorganic ions in several matrices; multivariate calibration methods for the quality control of pharmaceutical products and development of analytical methodology using solid-phase spectrometry.

**Luis F. Capitan-Vallvey**, Full Professor of Analytical Chemistry at the University of Granada, received his BSc in Chemistry (1973) and PhD in Chemistry (1986) from the Faculty of Sciences, University of Granada (Spain). In 1983, he founded the Solid Phase Spectrometry group (GSB) and in 2000, together with Prof. Palma López, the interdisciplinary group ECsens, which includes Chemists, Physicists and Electrical and Computer Engineers at the University of Granada. His current research interests are the design, development and fabrication of sensors and portable instrumentation for environmental, health and food analysis and monitoring. Recently is interested in printing chemical sensor and capillary-based microfluidic devices.

**Alberto J. Palma** received the BS and MSc degrees in physics in 1991 and the PhD degree in 1995 from the University of Granada, Granada, Spain. He is currently full professor at the University of Granada in the Department of Electronics and Computer Technology. Since 1992, he has been working on trapping of carriers in different electronic devices (diodes and MOS transistors) including characterization and simulation of capture cross sections, random telegraph noise, and generation-recombination noise in devices. From 2000 in the interdisciplinary group ECsens, his current research interests are devoted to design, development and fabrication of sensors and portable electronic instrumentation for environmental, biomedical and food analysis and monitoring. Recently he is working on printing sensors on flexible substrates with processing electronics using inkjet and screen-printing technologies.